Reflectance-based calibration of SeaWiFS. I. Calibration coefficients

Robert A. Barnes and Edward F. Zalewski

We present a calibration approach for the Sea-Viewing Wide Field-of-View Sensor (SeaWiFS) based on the reflectance properties of the instrument's onboard diffuser. This technique uses SeaWiFS as a reflectometer, measuring the reflected solar irradiance from the Earth and from the onboard diffuser. Because the Sun is the common source of light for both measurements, the ratio of the SeaWiFS-measured radiances from the Earth and the diffuser provide the ratio for the reflectances of the two samples. The reflectance characterization of the onboard diffuser is the calibration reference for this approach. Knowledge of the value of the solar irradiance is not required for these measurements because it falls out of the ratio. Knowledge of the absolute calibration coefficient for the SeaWiFS measurements of each of the two samples is not required either. Instead, the result of the ratioing technique is based on the linearity of the instrument's response to the intensity of the input light. The calibration requires knowledge, however, of the reflectance of the onboard diffuser at the start of the SeaWiFS mission and the response of the instrument bands, in digital numbers, for measurements of the diffuser at that time.

OCIS codes: 120.0120, 120.0280, 120.5700, 120.5630.

1. Introduction

The Sea-Viewing Wide Field-of-View Sensor (SeaWiFS) measures the upwelling Earth flux at wavelengths from 412 to 865 nm. Over this wavelength range, the flux comes from scattered sunlight. When the external light source is missing, such as on moonless nights, the Earth is essentially black in the visible and near infrared, except for anthropogenic illumination sources. Basically, the Earth behaves as a diffuse reflector for sunlight over these wavelengths, although the individual parts of this process can be quite complicated. This is the basis for the concept of remote sensing reflectance,[1,2] which is fundamental to measurements over the SeaWiFS wavelengths. For example, ocean chlorophyll is derived from a reflectance measurement, that is, from a measurement of scattered solar flux by phytoplankton after absorption by chlorophyll. In addition, properties of the land and atmosphere over these wavelengths are determined by remote sensing reflectance.

SeaWiFS measures the upwelling Earth flux as radiance because the Earth overfills the field of view of each SeaWiFS measurement. Thus SeaWiFS was calibrated in the laboratory with a large-aperture integrating sphere as a source of known radiance.[3] SeaWiFS measurements on orbit are tied directly to this laboratory source.[4] However, alternative calibration techniques by use of the Sun as the light source are possible. For example, the ground-based prelaunch calibration of SeaWiFS was performed outdoors,[5,6] where reflected sunlight from the SeaWiFS onboard diffuser provided the calibrated source of radiance. This calibration required knowledge of the reflecting properties of the SeaWiFS diffuser plus knowledge of the absolute value of the solar irradiance at the instrument's input aperture.

In addition, it is possible to calibrate SeaWiFS by use of the reflecting properties of the SeaWiFS diffuser without knowledge of the magnitude of the solar irradiance. This is the reflectance-based calibration of SeaWiFS. When this calibration is applied, SeaWiFS operates as a reflectometer, viewing the reflected solar flux from both the Earth and the onboard diffuser. Because the Sun is the common source of irradiance for both diffuse reflectors, the ratio of the two SeaWiFS measurements is also the ratio of the two reflectances. The reflectance-based

R. A. Barnes (rbarnes@seawifs.gsfc.nasa.gov) is with Science Applications International Corporation, Beltsville, Maryland 20705. E. F. Zalewski is with the Optical Science Center, Remote Sensing Group, University of Arizona, Tucson, Arizona 85721.

Received 30 August 2002; revised manuscript received 23 December 2002.

0003-6935/03/091629-19$15.00/0

calibration of SeaWiFS allows the direct determination of the remote sensing reflectance of the Earth, relative to the reflectance of the SeaWiFS onboard diffuser. It does not require knowledge of the absolute value of the flux from either the Sun or from an integrating sphere in the laboratory. However, the reflectance-based calibration does require the solar flux to be constant during the time between the two measurements in the ratio. This appears to be the case. Frölich[7] shows the solar constant to vary by approximately 0.2% over the course of a 22-year solar cycle. In addition, the reflectance-based calibration does not require knowledge of the calibrated radiances for the SeaWiFS measurements because the measurements are applied as a ratio. Instead, it is sufficient to know that the instrument output, in digital numbers (DNs), is a linear function of the input radiance as shown in Barnes *et al*.[8] Of course, it is also necessary to know other instrument characteristics, such as the relative spectral response.[4]

The reflectance-based calibration has three basic parts. The first is the laboratory characterization of the bidirectional reflectance distribution function (BRDF) of the onboard diffuser for the eight SeaWiFS bands. This is a system-level characterization of the diffuser and the diffuser assembly by use of an external light source and a pressed polytetrafluoroethylene (PTFE) diffuser as the calibration reference, as described in Section 3. The second part is the determination of changes, if any, in the diffuser BRDF from the time of the laboratory characterization to the start of the instrument's on-orbit operations. This is described in Section 4. The final part is the determination of diffuser changes since the start of on-orbit operations. This is described in Section 5. In addition, in Section 5 we describe the calculation of the eight instrument outputs, in DNs, at the start of the SeaWiFS mission. These values are an integral part of the reflectance-based calibration coefficients (see Section 7). In Sections 4 and 5 we use both system-level characterizations of the diffuser–diffuser assembly, with the Sun providing the input irradiance and the SeaWiFS instrument measuring the output radiance.

2. Instrument Description

SeaWiFS is an eight-band filter radiometer designed to monitor Earth-exiting radiances from ocean scenes. The nominal center wavelengths for the SeaWiFS bands are given in Table 1. The sensor's instantaneous field of view is 1.6 mrad by 1.6 mrad per pixel, with one scan covering 58.3° on either side of nadir. From a measurement altitude of 705 km, this gives Earth measurements, at nadir, that are 1.1 km on a side. SeaWiFS can be set to +20°, 0°, or −20° from nadir in the direction of flight to minimize the effects of ocean glint on the data. Each measurement is digitized to 10 bits, with a typical signal level of 600 DNs and a noise of 1 DN or less. The results of the prelaunch characterization of SeaWiFS are summarized in Barnes *et al*.[8]

SeaWiFS consists of a scanner, which contains the optics, detectors, preamplifiers, and scan mechanisms, and the electronics module, which contains the signal conditioning, command and telemetry, and power supply electronics. The SeaWiFS scanner is illustrated in Fig. 1. Light first strikes the primary mirror, an off-axis parabola, and then is reflected from a second surface polarization scrambler and from the half-angle mirror before reaching the field stop. The telescope primary mirror and the polarization scrambler are mounted on a cylinder that rotates six times per second. Both the telescope mirror and the entrance aperture on the cylinder have diameters of 10 cm. The half-angle mirror removes the rotation of the image from the scan of the telescope. It rotates at exactly half the rate of the telescope and polarization scrambler and uses alternating sides on successive telescope scans. The field stop, located at the entrance to the aft optics, is 50% larger than the detectors and restricts light through the system. After the field stop, the light is collimated by another off-axis paraboloid and directed to the aft optics assembly. Dichroic beam splitters in the aft optics divert the light into four focal-plane assemblies, each containing two spectral bands delineated by narrowband interference filters

Table 1. Nominal Center Wavelengths for the SeaWiFS Bands

Band	Nominal Center Wavelength (nm)
1	412
2	443
3	490
4	510
5	555
6	670
7	765
8	865

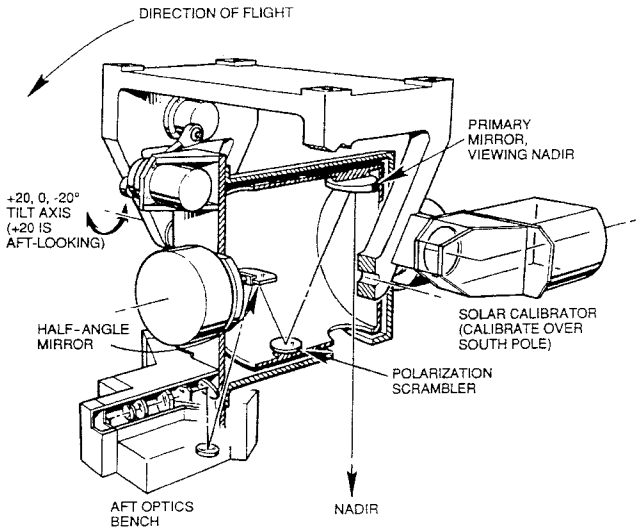

Fig. 1. Illustration of the SeaWiFS scanner. The solar diffuser (solar calibrator) assembly is pointed aft of the spacecraft's direction of flight.

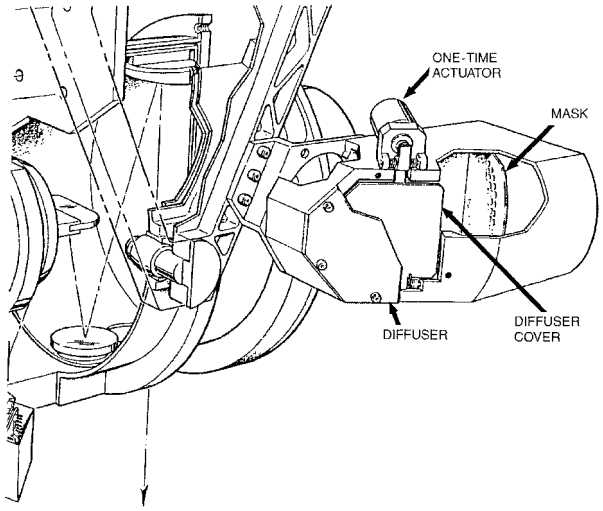

Fig. 2. Illustration of the solar diffuser assembly mounted to the SeaWiFS scanner.

in close proximity to the detectors. The measurements from the eight bands are acquired simultaneously and are coregistered on the Earth's surface to within one-half pixel.[8]

Two instrument bands, each with four detectors aligned in the scan direction, form a focal plane. Consequently, a point at the ground is seen successively by the four detectors. The outputs from the four detectors in each band are added by a time delay and integration technique to improve the signal-to-noise ratios. The signal from each detector is amplified, processed through a selectable gain stage, and digitized with a 12-bit analog-to-digital converter. The four digital outputs from a band are appropriately delayed, summed to obtain the digital-to-noise advantage, truncated to 10 bits, and transmitted to the ground by the Orbview-2 spacecraft. Use of time delay and integration has improved the signal-to-noise ratios of the SeaWiFS measurements by approximately a factor of 2. It is used in place of electronic averaging devices, such as integrating capacitors, which can also serve to improve signal-to-noise ratios. In addition, the time delay and integration design feature has been used to give SeaWiFS the ability[3,9] to make measurements of land and bright clouds, in addition to measurements of the oceans, which are significantly darker.

Measurements of the Sun are made with the primary telescope mirror rotated 90° from nadir (see Fig. 1). The solar diffuser (also called the solar calibrator) is pointed aft of the sensor's direction of flight. The diffuser views the Sun as the spacecraft passes over the Earth's South Pole because the spacecraft has a descending equatorial crossing. A baffle at the entrance of the diffuser assembly limits the field of view to ±11°, minimizing the diffuser's exposure to the solar flux. Figure 2 is an illustration of the diffuser assembly mounted to the SeaWiFS scanner. Here the primary telescope is aligned for a nadir view. Also in Fig. 2, sunlight enters the diffuser assembly from the right. The sunlight passes through the attenuator plate (also called the mask) and is scattered off the diffuser before entering the instrument to the left. The diffuser plate itself is part of the diffuser housing. It is painted on the inside surface of the housing, behind the diffuser cover in Fig. 2. Figure 2 shows the back of the diffuser cover, which is also painted and acts as a secondary diffuser. The cover has a spring-loaded hinge at its bottom and is held in the vertical position by a solenoid actuator. When the one-time actuator releases the cover, the diffuser cover rotates into the page and comes to rest on the bottom of the housing. The diffuser has a nominal illumination angle of 60° to avoid specular glints from its surface and to reduce the flux density on the diffuser plate by a factor of 2. The plate and the diffuser cover both have coatings of YB-71 paint. The wavelength dependence of the reflectivity of a YB-71-coated plate is essentially flat over the wavelength range of the SeaWiFS bands.[10]

The attenuator is a flat-black anodized aluminum aperture plate with holes that reduce the solar flux on the diffuser. The hole size, 1.0 mm in diameter, and the spacing of the holes, 2.5 mm between centers in a grid pattern, ensure that images of the Sun partially overlap on the diffuser, providing a uniformly illuminated surface. The pattern of the aperture holes is rotated 35° with respect to the Sun's path across the diffuser to reduce striping of the diffuser by photolyzed contaminants over the lifetime of the SeaWiFS mission. The distance between the attenuator plate and the diffuser is such that reflections from the back of the attenuator onto the diffuser account for less than 1% of the total illumination.

The attenuator plate has a uniform thickness of 2.5 mm and is tilted by 30° from the entrance plane of the diffuser housing. This design reduces the glint from the attenuator plate on the diffuser, and it reduces the illumination variations as the incidence angle of the Sun changes over the seasons.[11] Over each SeaWiFS orbit, the instrument rotates (pitches) through 360°. However, because of the inclination of the Earth's axis to the plane of the Earth's orbit and because of the inclination of the satellite's orbit about the Earth, there is also a relative motion of the solar incidence angle in one of the axes normal to the rotation in pitch (the yaw axis). This motion has a range of approximately ±6°, and it is the change in the transmission of the attenuator plate over this angular range that the tilted attenuator plate reduces[11] (see Fig. 3). Overall, the effective BRDF of the SeaWiFS diffuser is smaller than that of the PTFE diffuser by approximately a factor of 10.

As discussed here, the SeaWiFS instrument and the Orbview-2 spacecraft are described in Cartesian coordinates, that is, in terms of their x, y, and z axes. For measurements of the Earth, the nadir view of the Earth is in the $+x$ direction, and the instrument flies along its orbital trajectory in the $+y$ direction. Nadir pointing is accomplished when the orientation of the instrument plane (the y, z plane) that is normal to the nadir (the $+x$) direction is maintained. To main-

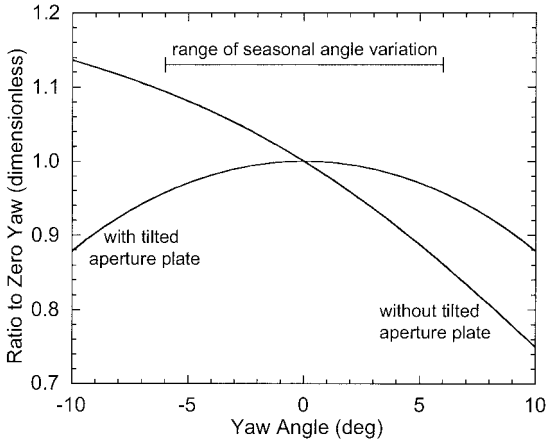

Fig. 3. Diffuser attenuator plate performance characteristics as predicted at the SeaWiFS Critical Design Review on 18 and 19 December 1991.[11] The solar yaw angles were predicted to have a range on orbit of approximately ±6° about zero yaw at the input aperture of the diffuser assembly. At ±6°, the transmittance of the attenuator plate was predicted to be approximately 96% of that at zero yaw.

tain nadir pointing throughout the orbit, the spacecraft pitches (rotates about the z axis) through 360°, while the spacecraft roll (rotation about the y axis) remains fixed. Alignment along the orbital trajectory is accomplished when the instrument plane (the x, z plane) that is normal to the spacecraft flight (the $+y$) direction is maintained. To maintain this orientation, the spacecraft yaw (rotation about the nadir-pointing axis) also remains constant.

The input aperture for the SeaWiFS diffuser assembly is part of the x, z plane at the aft of the instrument. In this orientation, the input aperture is normal to spacecraft's $-y$ axis. For the laboratory characterization of the SeaWiFS diffuser assembly (see Section 3), the irradiance source was aligned with the instrument's $-y$ axis. In other words, the pitch and yaw angles were both set to zero. For measurements on orbit, the solar irradiance must also be aligned with the spacecraft's $-y$ axis. And for solar measurements, it is possible to select the time of the measurement so that the pitch angle is close to zero. However, the yaw angle relative to the Sun can vary by ±6° over the course of each year. This variation is a consideration in the design of the attenuator plate. It is also a consideration in the determination of diffuser changes on orbit (see Section 5).

3. Laboratory Measurements

The laboratory characterization of the SeaWiFS diffuser has been described previously,[12] including the complete measurement equation for reflectance. In summary, that characterization is based on the simplified reflectance equation,

$$F_\lambda(\phi_I, \theta_I) = \frac{L_\lambda}{E_\lambda \cos(\theta_I)}, \quad (1)$$

where $F_\lambda(\phi_I, \theta_I)$ is the BRDF at wavelength λ for a fixed set of scattering angles and where ϕ_I and θ_I are the incident azimuthal and zenith angles, respectively. The units for the BRDF are inverse steradians, and the zenith angle is given with respect to the normal to the scattering surface. In Eq. (1), L_λ is the scattered spectral radiance at wavelength λ, and E_λ is the incident spectral irradiance. For the SeaWiFS Project, the units for spectral radiance (L_λ) are mW cm^{-2} sr^{-1} μm^{-1} and the units for spectral irradiance (E_λ) are mW cm^{-2} μm^{-1}. The term $\cos(\theta_I)$ is the effect of the projection of the incident radiation when it is not normal to the surface. This applies whenever the illuminated area on the surface overfills the field of view of the instrument that measures the reflected radiation.

The angles in Eq. (1) are given in polar coordinates. This is the standard formalism for BRDF measurements, and this is the formalism used in this section and Section 4. However, the laboratory characterization of the SeaWiFS diffuser and the SeaWiFS solar measurements on orbit are both made in terms of the instrument's Cartesian coordinate system. There is an angular transformation between the spacecraft's Cartesian coordinates and the polar coordinates from Eq. (1). However, it is not necessary to know that transformation if a consistent coordinate system is maintained for all SeaWiFS diffuser measurements.

The characterization of the SeaWiFS diffuser is based on Eq. (1). The end-to-end system-level characterization by the instrument manufacturer connected the instrument response for views of the diffuser to the instrument response for views of the Earth at instrument nadir. Determining the diffuser reflectance required two measurements. For the first measurement, the diffuser was illuminated normal to its input aperture with a source having an angular subtense similar to that of the Sun. The illumination source was a 1000-W FEL-type lamp placed approximately 300 cm from the instrument. For this measurement, the output from SeaWiFS gave the radiance scattered from the onboard diffuser.

In the second measurement, SeaWiFS was rotated to measure the reflected light from a second, external diffuser as if the instrument were viewing the Earth. The external diffuser was a pressed PTFE sample with a known BRDF.[13] In this measurement, the irradiance from the FEL lamp was normal to the PTFE surface, and SeaWiFS measured the scattered radiance at an angle of 45° from normal. For this measurement configuration, the cosine of the incident irradiance on the external PTFE diffuser was unity. Both laboratory measurements were made on the same day, and for both measurements, the lamp–diffuser distance was the same. For the first measurement, the distance was measured from the lamp to the input aperture of the SeaWiFS diffuser assembly. Because both SeaWiFS measurements used the same irradiance source at the same distance, the ratio of these two measurements is the

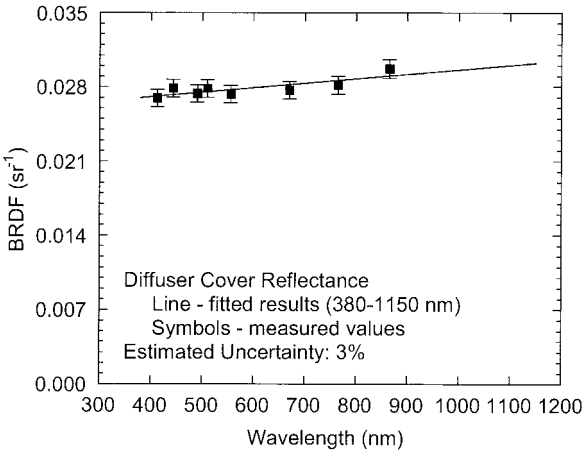

Fig. 4. Reflectances for the eight SeaWiFS bands. The estimated uncertainty for these measurements is 3%. See text for details.

ratio of the BRDF of the SeaWiFS diffuser to that of the PTFE diffuser.

For the laboratory characterization of the SeaWiFS diffuser, the scattered radiance from the onboard diffuser included instrumental factors, such as possible scattered light within the instrument cavity and the specific, nonnormal angle of the irradiance on the instrument diffuser itself. For the PTFE diffuser the angles of incidence and reflection were those used by Hsia and Weidner,[14] 0° and 45°. They measured the BRDF of pressed PTFE to be 0.321 sr^{-1} at 550 nm. At other wavelengths, the BRDF of PTFE is obtained when the 550-nm value is multiplied by the relative (that is, the 550-nm normalized) 6-deg/hemispherical spectral reflectance.[13] Over the wavelength range of SeaWiFS bands 3–8 (490, 510, 555, 670, 765, and 865 nm), the spectral reflectance of pressed PTFE is constant. For bands 1 and 2 (412 and 443 nm), the reflectance decreases by 0.1%.

As described above, the SeaWiFS instrument has two diffusers, with the second diffuser on a cover plate over the first. After more than four years on orbit, the cover remains in place, acting as the primary flight diffuser. The changes in the cover have been reasonably small (see Section 5), and it continues to function adequately. There were no laboratory measurements of the reflectance of the diffuser cover; however, during the ground measurements of the Sun with the diffuser,[5] the counts from the instrument were taken by use of the cover with the solar irradiance normal to the input aperture of the diffuser assembly. Immediately afterwards, the diffuser cover was rotated out of the optical path, and the counts from the instrument were taken with the diffuser. The ratios of the diffuser cover counts to the diffuser counts and the laboratory measurements of the diffuser BRDF were used to calculate the diffuser cover BRDF values.[6] The BRDF values for the diffuser cover are close to those for the diffuser itself.[6] The diffuser cover BRDF values, as presented in Barnes *et al.*,[6] are shown in Fig. 4. Figure 4 also includes 3% uncertainty estimates for the reflectance values for the SeaWiFS bands. As with all other uncertainties for the calibration of SeaWiFS, these values are given for $k = 1$ (for one sigma).

The uncertainty for the reflectance measurements by the instrument manufacturer is difficult to assess. In a round-robin comparison of BRDF measurements,[15] the manufacturer's measurements of a pressed PTFE sample agreed with the National Institute of Standards and Technology values at an uncertainty level ($k = 1$) of less than 1%. This comparison was performed several years after the calibration of SeaWiFS. However, it does represent the state of the art for reflectance measurements by an instrument manufacturer. For SeaWiFS, we have expanded this state-of-the-art uncertainty to 3% to account for alignment uncertainties in the laboratory calibration of the diffuser and for uncertainties in the transfer of the diffuser BRDF to the diffuser cover. In addition, the 3% uncertainty is the same as that for the radiance-based calibration of SeaWiFS in the laboratory.[4]

The SeaWiFS diffuser assembly was characterized at the system level in the laboratory by an external irradiance source and an external reference diffuser. This characterization was done with the irradiance normal to the plane of the diffuser assembly's entrance aperture. A partial characterization of two SeaWiFS bands (bands 4 and 8) at other irradiance incidence angles was performed by the instrument manufacturer.[10] However, a complete characterization of the angular dependence for all eight bands was not required for compliance with the instrument's performance specifications,[8] so the angular characterization that is required for the reflectance-based calibration was performed on orbit (see Section 5).

4. Transfer-to-Orbit Experiment

SeaWiFS carries no internal reference source that can be measured before and after launch to detect calibration changes during the period between the laboratory calibration of the instrument and the start of on-orbit operations. For the SeaWiFS Project, the Sun is used as an external reference source, measured at the manufacturer's facility and again after launch, to detect instrument changes during this period. This is the SeaWiFS transfer-to-orbit experiment.

The experiment has been described previously,[12] so only a summary is presented here. In the transfer-to-orbit experiment, measurements of the solar irradiance are made from the ground before launch. With these measurements, the initial on-orbit response of the instrument, when viewing the Sun, is predicted. The difference between the predicted and the actual response on orbit gives a measure of the change in the instrument. Because the onboard diffuser is required for these measurements, the experiment measures the change in the instrument–diffuser system. There is no mechanism in this

experiment to separate changes in the diffuser from changes in the instrument.

Geometric factors, primarily the incidence angles of the solar irradiance on the instrument during the two phases, are important. However, the experiment hinges on the quality of the atmospheric transmission measurements during the ground portion of the experiment because the atmosphere is the primary difference in the two experiment parts.

The solar measurements are based on the BRDF of the SeaWiFS diffuser, which is defined in Eq. (1). For the transfer-to-orbit experiment, E_λ is the spectral solar irradiance incident on the diffuser, and θ_I is the incidence angle of the solar irradiance on the entrance aperture of the diffuser assembly. The incident irradiance for a solar measurement is calculated from a solar model and the Earth–Sun distance:

$$E_\lambda = \frac{E_{M,\lambda}}{D_{\mathrm{ES}}{}^2}, \tag{2}$$

where $E_{M,\lambda}$ is the model irradiance at a distance of 1 astronomical unit (AU) and D_{ES} is the Earth–Sun distance (in AU).

For SeaWiFS, the relationship between the output of the instrument and the input spectral radiance is defined as

$$L_\lambda = (\mathrm{DN} - \mathrm{DN}_0)k_2(g), \tag{3}$$

where the value of the DNs for the input radiance is DN, the value of the DNs for an input radiance of zero radiance is DN_0, the calibration coefficient is $k_2(g)$, g is the electronic gain for the measurement, and the calculated spectral radiance is L_λ. The units for the calibration coefficient are in terms of spectral radiance per DN (mW cm^{-2} sr^{-1} $\mu\mathrm{m}^{-1}$ DN^{-1}). Equations (1)–(3) can be combined to give the equation for a SeaWiFS solar diffuser measurement at wavelength λ:

$$(\mathrm{DN} - \mathrm{DN}_0) = \frac{L_\lambda}{k_2(g)} = \frac{E_{M,\lambda}F_\lambda(\phi_I, \theta_I)\cos(\theta_I)}{D_{\mathrm{ES}}{}^2 k_2(g)}. \tag{4}$$

With finite spectral bandwidths, SeaWiFS can provide only an approximation to the spectral radiance at a single wavelength. For SeaWiFS, the spectral radiance from the measurement is approximated by the band-averaged spectral radiance.[4] In the SeaWiFS radiometric calibration equation, the calibration coefficient $k_2(g)$ is defined in terms of the band-averaged spectral radiance:

$$k_2(g) = \frac{L_B}{(\mathrm{DN} - \mathrm{DN}_0)} = \frac{\displaystyle\int_{\lambda_1}^{\lambda_2} L_\lambda R_\lambda \mathrm{d}\lambda}{\displaystyle\int_{\lambda_1}^{\lambda_2} R_\lambda \mathrm{d}\lambda} \Big/ (\mathrm{DN} - \mathrm{DN}_0), \tag{5}$$

where L_B is the band-averaged spectral radiance with units of mW cm^{-2} sr^{-1} $\mu\mathrm{m}^{-1}$, R_λ is the spectral response of the band, and λ_1 and λ_2 are the lower and upper limits of integration. These wavelengths are 380 and 1150 nm, respectively. They are the wavelengths over which the SeaWiFS photodiodes have a significant quantum efficiency.[9] The ratio of integrals in Eq. (5) gives the definition of the band-averaged spectral radiance.

For measurements of the solar irradiance at the top of the atmosphere (TOA) at the start of on-orbit operations, the output from each instrument band is

$$(\mathrm{DN} - \mathrm{DN}_0)_{\mathrm{TOA}} = \frac{\cos(\theta_I)}{D_{\mathrm{TOA}}{}^2 k_2(g_{\mathrm{TOA}})} \times \frac{\displaystyle\int_{\lambda_1}^{\lambda_2} E_{M,\lambda}F_\lambda(\phi_I, \theta_I)R_\lambda \mathrm{d}\lambda}{\displaystyle\int_{\lambda_1}^{\lambda_2} R_\lambda \mathrm{d}\lambda}. \tag{6}$$

Equation (6) is a modification of Eq. (4), with the band-averaged spectral radiance substituted for the spectral radiance at a single wavelength and with the Earth–Sun distance and the instrument gain set to that for the TOA measurement. For measurements on the ground (GND) before launch, the calculation of the output from each band is nearly the same:

$$(\mathrm{DN} - \mathrm{DN}_0)_{\mathrm{GND}} = \frac{\cos(\theta_I)}{D_{\mathrm{GND}}{}^2 k_2(g_{\mathrm{GND}})} \times \frac{\displaystyle\int_{\lambda_1}^{\lambda_2} E_{M,\lambda}F_\lambda(\phi_I, \theta_I)T_\lambda R_\lambda \mathrm{d}\lambda}{\displaystyle\int_{\lambda_1}^{\lambda_2} R_\lambda \mathrm{d}\lambda}. \tag{7}$$

However, Eq. (7) contains the transmittance of the solar flux through the atmosphere T_λ (dimensionless). The atmospheric transmittance spectrum is shown in Fig. 5. The transmittance measurements were made with a solar radiometer possessing ten bands covering the spectral range of approximately 370–1140 nm. On the basis of calibrations of the solar radiometer done before and after the transfer-to-orbit experiment, it is expected that the error in the atmospheric transmittances was approximately 3% or less at the measurement wavelengths.[12] Along with the measured barometric pressure at the ground, these transmittances were used to calculate the atmospheric transmittance spectrum at 1-nm intervals from 380 to 1150 nm, which is the wavelength range of the SeaWiFS spectral response measurements.

For the ground measurements, there was also light from the sky illuminating the diffuser. We measured the amount of this light by blocking the direct solar flux using a disk that was supported over the diffuser.[12] Finally, during the ground measurements, the instrument was aligned so that the solar irradiance was normal to the input aperture of the

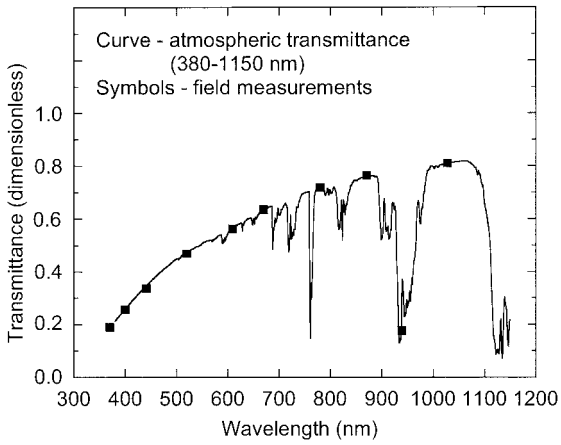

Fig. 5. Atmospheric transmittances during the ground portion of the transfer-to-orbit experiment. The symbols give the measurements from the sunphotometer. The curve gives the derived atmospheric transmittance spectrum.

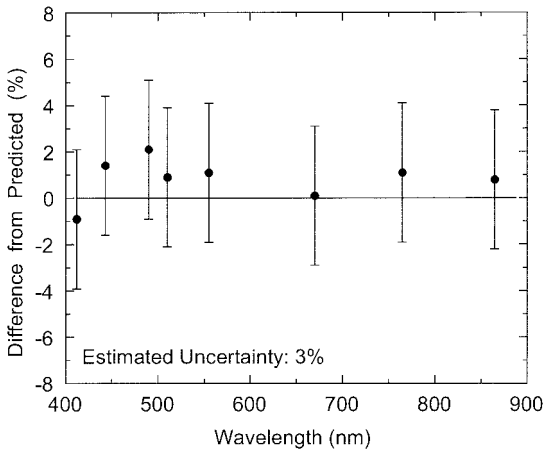

Fig. 6. Results of the transfer-to-orbit experiment for the eight SeaWiFS bands. These are the differences of the on-orbit measurements of the Sun from those predicted from the ground measurements prelaunch. At the 3% level, there is no sign of change in the reflectance of the SeaWiFS diffuser from its laboratory characterization to the start of on-orbit operations.

diffuser. This allows the removal of the cosine of the zenith angle from the ratio of Eq. (6) to Eq. (7):

$$\frac{(\mathrm{DN} - \mathrm{DN}_0)_{\mathrm{TOA}}}{(\mathrm{DN} - \mathrm{DN}_0)_{\mathrm{GND}}} = \frac{D_{\mathrm{GND}}{}^2 k_2(g_{\mathrm{GND}})}{D_{\mathrm{TOA}}{}^2 k_2(g_{\mathrm{TOA}})} \times \frac{\int_{\lambda_1}^{\lambda_2} E_{M,\lambda} F_\lambda(\phi_I, \theta_I) R_\lambda \mathrm{d}\lambda}{\int_{\lambda_1}^{\lambda_2} E_{M,\lambda} F_\lambda(\phi_I, \theta_I) T_\lambda R_\lambda \mathrm{d}\lambda}. \quad (8)$$

When we use the net counts from each band during the ground measurements $(\mathrm{DN} - \mathrm{DN}_0)_{\mathrm{GND}}$, it is possible to predict the net counts from each SeaWiFS band at the TOA at the start of SeaWiFS operations on orbit. This prediction requires knowledge of the Earth–Sun distance and use of a solar model ($E_{M,\lambda}$). The choice of the model has little effect on the prediction because it is found in both integrals in Eq. (8). However, the atmospheric transmittance T_λ is found only in the denominator of the equation. It is the major source of uncertainty in the transfer-to-orbit experiment.

The remaining terms in Eq. (8) come from the SeaWiFS band: the BRDF of the diffuser, the spectral response of the band, and the gain coefficients. To predict the net DNs at the TOA, it is assumed that these terms do not change. Figure 6 shows the ratios of the actual DNs from the SeaWiFS bands to the values predicted from the ground measurements. The mean value for these ratios is 1.013 and the standard deviation is 0.012.[12]

There are four uncertainties in the transfer-to-orbit experiment.[12] The first is the uncertainty in the atmospheric transmittances for the ground measurements, which is approximately 3%. The second is the uncertainty in the calculation of the amount of diffuse light blocked by the occulting disk during the ground measurements, which is estimated at approximately 0.25% of the DNs from that part of the experiment. The third is the uncertainty in the diffuser reflectance for the two parts of the experiment. This does not arise from the absolute value for the reflectance but from the difference in the angle of the solar irradiance for the two parts of the experiment. For the ground portion, the alignment was within 0.25° of the normal to the input aperture of the diffuser housing. For the measurements on orbit, the difference was within 2°. For the SeaWiFS diffuser, this leads to a change of approximately 0.5% in the BRDF for the two parts.

The fourth uncertainty arises from the correction for the changes in the instrument–diffuser system from the launch of SeaWiFS to the date of the first measurements of the Sun.[12] The corrections for these changes are approximately 1–2%. Because an extrapolation is required to determine these changes, the uncertainty in the corrections is estimated to be 1%. For the four uncertainties, the square root of the sum of the squares is approximately 3.2%. However, it is clear that the overall uncertainty is not known at the 0.10% percent level, so the uncertainty estimate for the experiment is set at 3%, which is the value of the principal uncertainty source.

For the SeaWiFS radiance-based calibration on orbit,[4] the results of the transfer-to-orbit experiment in Fig. 6 are not applied as corrections to the prelaunch calibration coefficients. Rather the 3% uncertainty from the experiment is combined with the 3% uncertainty from the prelaunch radiometric calibration to give an estimate of the uncertainty in the radiance-based calibration coefficients at the start of on-orbit operations. However, there is no mechanism in the transfer-to-orbit experiment to separate changes in the diffuser from changes in the instrument. In this regard, the transfer-to-orbit experiment works equally well to estimate the uncertainty in the reflectance of the SeaWiFS diffuser at the start of the

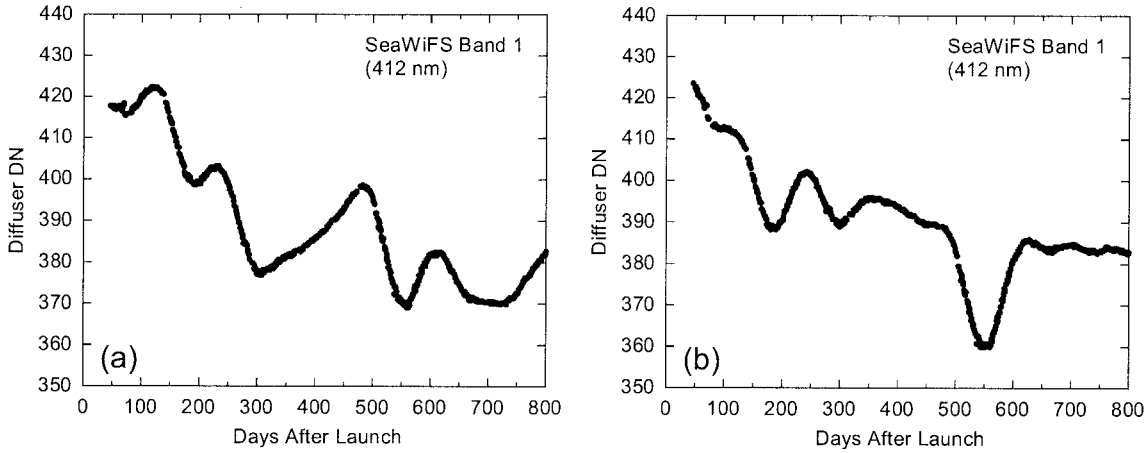

Fig. 7. Solar diffuser measurements for SeaWiFS band 1. The measurements are made on a nearly daily basis. They are given as DNs. (a) Uncorrected measurements of the diffuser. (b) Measurements corrected for the Earth–Sun distance and for the temperature dependence of the focal plane for SeaWiFS band 1. The distance correction is to 1 AU and the temperature correction is to 20 °C.

SeaWiFS mission. For the diffuser, the 3% uncertainty in the laboratory characterization of the BRDF is combined with the 3% uncertainty in the transfer-to-orbit to estimate the uncertainty in the diffuser BRDF at the start of on-orbit operations.

5. Diffuser Changes on Orbit

Changes in the DNs from each SeaWiFS band during the diffuser measurements on orbit come from four sources: changes in the SeaWiFS instrument, changes in the Earth–Sun distance, changes in the incidence angle of the solar irradiance on the diffuser, and changes in the reflecting properties of the diffuser itself. A knowledge of the changes in the response of the instrument is fundamental to an understanding of the changes in the diffuser because the output from the solar diffuser measurements comes from the instrument–diffuser system. Long-term changes in the radiometric calibration of the SeaWiFS bands have been determined from measurements of the Moon.[4]

Of course, the knowledge of the changes in the diffuser can never be as good as that of changes in the instrument itself, so the time period for this study is limited to the initial set of SeaWiFS measurements on orbit when the changes in the instrument and the diffuser are still relatively small. Results are given for the first 400 days after the launch of SeaWiFS, which correspond to the first year of on-orbit Earth observations. For SeaWiFS, the orbit raising and outgassing period preceding Earth observations took 34 days. To obtain the 400-day results, the time series for the instrument and diffuser changes were measured over 800 days, twice the period for the results. This was done to provide fitted curves for the time series that extend beyond the 400-day study period so that the curves are well behaved at the end of the study period. This was been done to provide an extended set of cycles of the change of the yaw angle of the solar irradiance on the diffuser to allow a better determination of those angular effects.

SeaWiFS was designed without the incorporation of a device, such as a ratioing radiometer,[16] to provide an independent determination of the time-dependent changes in the diffuser. Thus the solar measurements are made with the instrument–diffuser system, and the change in the diffuser over time can be determined no better than the change in the instrument itself.

In this section, the contributing factors to the time-dependent changes in the solar diffuser measurements are removed from the measurement set until the changes in diffuser reflectance remain alone in the data set. The results here are shown for SeaWiFS band 1, which are equivalent to those for the other bands.

Figure 7(a) shows the uncorrected DNs for the solar diffuser measurements from SeaWiFS band 1. The values are uncorrected, except for the removal of the zero offset (DN_0). The offset is measured over part of each telescope rotation as the telescope views the black interior of the instrument housing. The data in Fig. 7(a) are plotted versus the time (in days) after the launch of SeaWiFS. There is a period of 45 days between the launch of the instrument and the first solar measurement. Figure 7(b) shows the DNs after the correction for the Earth–Sun distance and for the effect of temperature changes in the focal plane on the output of the band. Because the Sun underfills the field of view of the diffuser and the rest of the field of view is black, the amount of irradiance on the diffuser varies with the square of the Earth–Sun distance. The time dependence of the Earth–Sun distance (in AU) is know from astronomical almanacs, and the distance correction adjusts the DN from the diffuser measurement to that for the irradiance at a standard Earth–Sun distance of 1 AU. In addition, there is a direct connection between the Earth–Sun distance and the focal-plane temperature because the instrument is warmer when it is closer to the Sun.

Figure 8(a) shows the temperature of the focal

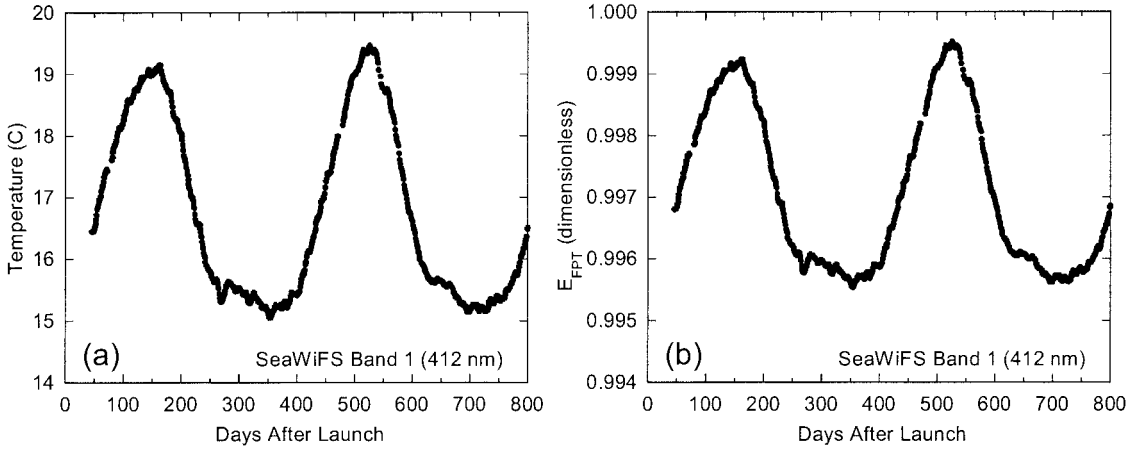

Fig. 8. Focal-plane temperature (FPT) effect for SeaWiFS band 1. The effect is calculated by Eq. (9). (a) Focal-plane temperature. (b) Focal-plane temperature effect.

plane for SeaWiFS band 1. For the other bands, the focal-plane temperatures are nearly identical to those in Fig. 8(a). The effect of the focal-plane temperature on the output of each SeaWiFS band is given by

$$E_{\mathrm{FPT}} = 1 + k_3(T - T_{\mathrm{REF}}), \tag{9}$$

where E_{FPT} is the effect of the dependence (dimensionless), k_3 is the dependence factor (C^{-1}), T is the focal-plane temperature (°C), and T_{REF} is the reference temperature for the laboratory measurements of the effect (20 °C).[9] The temperature-dependent correction is applied as the reciprocal of E_{FPT}. Each band has its own k_3 factor, ranging from 0.000901 $\mathrm{°C}^{-1}$ for band 1 to -0.001682 $\mathrm{°C}^{-1}$ for band 8. The focal-plane temperature effect for SeaWiFS band 1 is shown in Fig. 8(b). The effects for the other bands scale according to the magnitude of k_3.

For SeaWiFS measurements of the Earth, there is an additional instrument effect that involves the angle of incidence of the input radiance, relative to the angle of Earth measurements at nadir.[9] This effect is called scan modulation by the SeaWiFS Project. For the diffuser measurements presented here, the measurements are made at a fixed scan angle relative to nadir. And in the laboratory determination of the diffuser BRDF, the measurements of the SeaWiFS diffuser were referenced to the measurements of the PTFE diffuser located at the Earth nadir position. For these reasons, scan modulation is not part of the determination of the time-dependent changes in the reflectance of the diffuser–instrument system.

Long-term changes in the radiometric sensitivity of the SeaWiFS bands are determined by measurements of the Moon.[4] For SeaWiFS band 1, the change is given as an exponential curve that has a value of unity at the day of launch. The curve approaches a value of 0.988 at a time several years into the future. Each of the other SeaWiFS bands are also fitted to exponential curves, except for bands 3 and 4 (490 and 510 nm, respectively). It is assumed by the SeaWiFS Project that these bands change little over time, so they are fit to linear curves that are essentially constant with time.[4] The long-term time change in radiometric sensitivity for band 1 is shown in Fig. 9(a). This covers the first 800 days after launch. The fitted curves for the complete set of SeaWiFS bands are shown in Barnes *et al.*[4] At the time of this writing, the lunar measurement set extends beyond 1700 days from the launch of SeaWiFS. Figure 9(b) shows the values in Fig. 7(b) after their correction for the long-term change in the radiometric sensitivity of band 1. The correction is applied as the reciprocal of the exponential curve in Fig. 9(a).

The pitch and yaw angles of the solar irradiance at the input aperture of the diffuser housing are shown in Figs. 10(a) and 10(b). Because it is possible to time the diffuser measurements as the spacecraft passes over the Earth's South Pole, Fig. 10(a) shows the pitch angles for the measurements to be essentially zero. However, the yaw angles in Fig. 10(b) vary over the range of angles predicted in the prelaunch characterization of the instrument (see Fig. 3). As shown in Fig. 3, the yaw-angle dependence has a maximum at an angle near normal incidence (near zero degrees) on the diffuser assembly's input aperture.

With the removal from the data set of the other known effects causing cyclic changes of the order of one year (the Earth–Sun distance and the focal-plane temperatures), the yaw-angle dependence remains as the sole source of cyclic features in the time series. These features arise from the cyclic change in yaw angle on orbit, as shown in Fig. 10(b). For SeaWiFS, the measurements on orbit replace the partial, laboratory-based characterization of the BRDF in Barnes and Eplee.[10] As with the other characterizations of the SeaWiFS diffuser and diffuser assembly, the yaw-angle correction is performed at the system level, with the Sun as the source of input irradiance and the instrument as the monitor of changes in the output radiance. A determination of the pitch-angle dependence of the BRDF is not necessary because the diffuser measurements on orbit are constrained to a pitch angle of zero degrees.

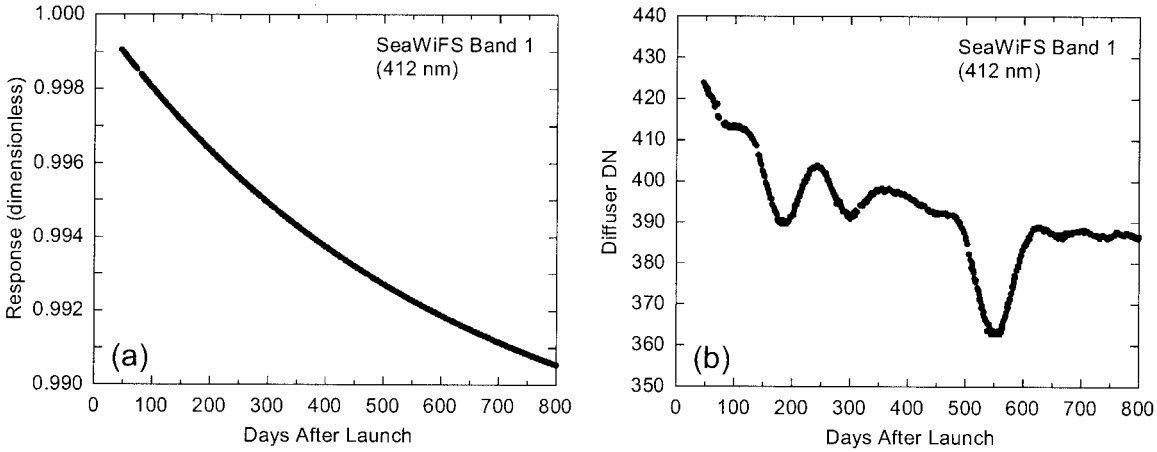

Fig. 9. Correction for the long-term changes in the radiometric sensitivity of SeaWiFS band 1. (a) Band 1 response normalized to unity on the day of launch.[4] (b) Diffuser measurements after the correction for the change in the instrument response. The measurements without the correction for this change are shown in Fig. 7(b).

The procedure to determine the yaw-angle correction starts when we find a set of measurements where the angular response is close to its maximum, that is, for a yaw angle close to zero. In this procedure, the angle for this response is −1.5°. A line through the set of yaw angles at −1.5° is shown in Fig. 11(a). It passes through the yaw curve several times, whereas a line at 0° passes through the curve fewer times.

Figure 11(b) shows the values from Fig. 9(b), including the data points where the yaw angles are −1.5°. Figure 11(b) also includes a cubic spline curve interpolating between the data points at −1.5° yaw. The cubic spline gives the best guess at the response of the diffuser measurement in the absence of the yaw-angle dependence. For dates preceding day 111 after launch, none of the data points intersect the −1.5° line. This makes spline interpolation for these data impossible, and they are removed from Fig. 11(b). Figure 12(a) gives the diffuser measurements in Fig. 11(b), normalized by the corresponding values of the fitted spline curve. These results are plotted in Fig. 12(a) versus the yaw angle of the measurement. The values in Fig. 12(a) form a shape that is close to the one in Fig. 3. This is an indication that the measurements on orbit follow the pattern predicted from the design of the instrument. In addition, Fig. 12(a) contains a fourth-order polynomial curve fitted to the data points (the curve is hidden by the data points). The polynomial curve, by itself, is shown in Fig. 12(b). This curve is the basis for the correction of the yaw-angle dependence for SeaWiFS band 1.

The change in the incidence angle of the solar flux with yaw angle is a contributor to the results in Fig. 12 because the image of the Sun on the diffuser overfills the field of view of the instrument. This contribution is small, however, because the cosine of 6° is 0.995.

The maximum values of the yaw-angle dependence curves for the eight SeaWiFS bands are listed in Table 2, which also includes the yaw angle for each maximum. In each case the angle falls within 1° of zero yaw. And in each case, the maximum value of the polynomial curve is slightly greater than unity but by less than 0.3%. For all the SeaWiFS bands, the yaw-angle responses presented here agree closely

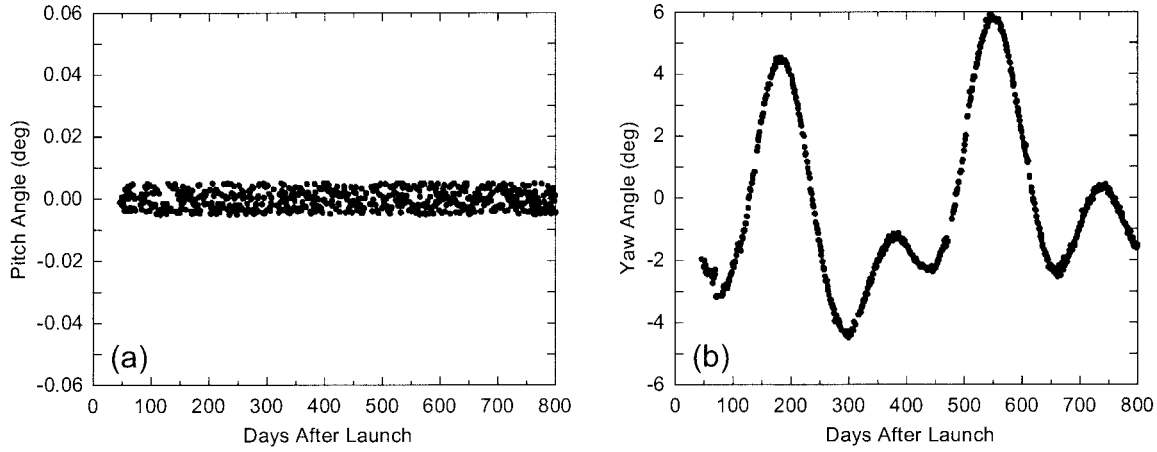

Fig. 10. (a) Pitch and (b) yaw angles for the measurement set.

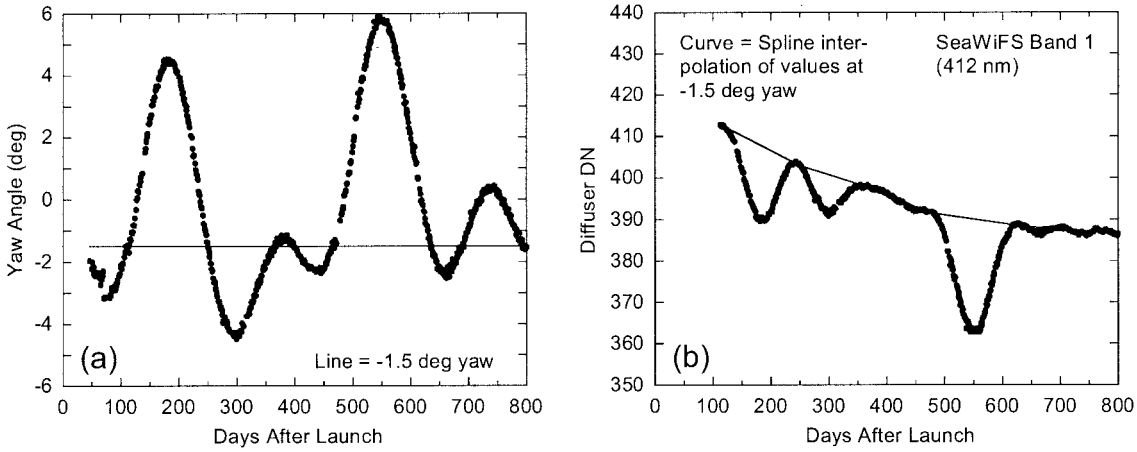

Fig. 11. Band 1 solar diffuser measurements at −1.5° yaw angle. There are eight days for which the yaw angles are −1.5°, from day 111 after launch to day 799 after launch. (a) Yaw angles for the measurement set. The line connects to values at −1.5° yaw. (b) Band 1 measurements from day 111 to day 799. These measurements come from Fig. 9(b). The curve gives the spline interpolation of the DN on the eight days for which the yaw angle is −1.5°.

with the response predicted at the SeaWiFS Critical Design Review[11] (see Fig. 3). The yaw-angle correction is applied when the polynomial curve is normalized to a maximum value of unity and the values in Fig. 9(b) are multiplied by the reciprocal of the resulting curve. This process is possible because each diffuser measurement has its own yaw angle.

The limitation of the pitch angles of the measurements to zero-degrees pitch and the correction of the yaw-angle effects back to zero-degrees yaw provide the response of the diffuser to illumination by the Sun normal to the plane of the entrance aperture of the diffuser assembly. This condition duplicates the angle of the incident flux during the laboratory characterization of SeaWiFS. In the laboratory calibration, a pressed PTFE diffuser was used as a calibration standard, and the SeaWiFS radiometer transferred that standard to the flight diffuser. On orbit, the conditions of the laboratory characterization have been duplicated, as closely as possible, and deviations from those conditions have been corrected, as closely as possible.

The resulting diffuser data set, shown in Fig. 13(a), gives the residual of the diffuser measurements after the effect of instrument changes, the Earth–Sun distance, and the yaw-angle dependence of the diffuser response were removed. With these effects removed, the changes in Fig. 13(a) come from the changes in the BRDF of the diffuser itself for SeaWiFS band 1. The fitted curve from Fig. 13(a), without the data points, is shown in Fig. 13(b).

For each of the SeaWiFS bands, the fitted curve for the change in the diffuser reflectance has two parts. The first part is derived from a first-order polynomial fit to the values from day 46 after launch to day 72 after launch. This is the procedure used in the

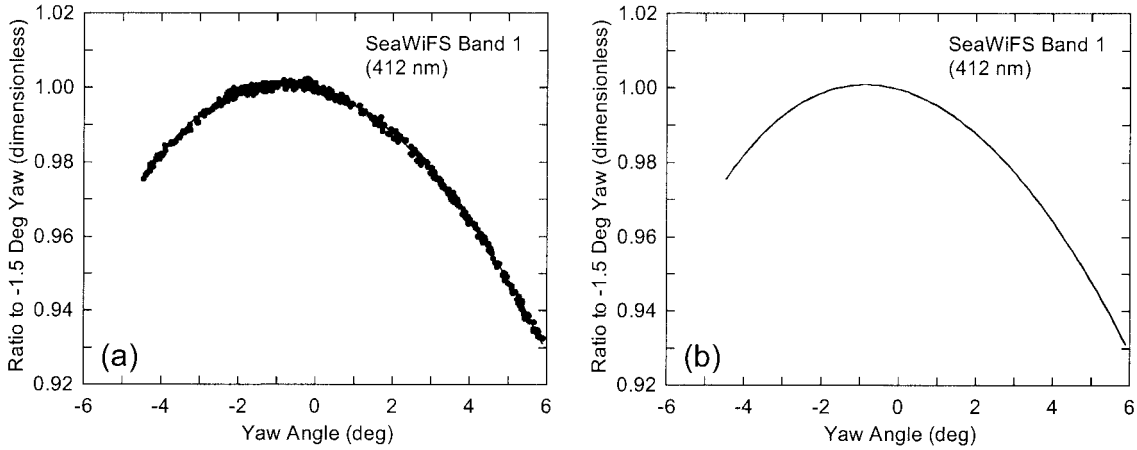

Fig. 12. Ratios of the band 1 diffuser measurements to the values at −1.5° yaw. The measurements for these plots come from Fig. 11(b). Because each measurement has its own yaw angle, the abscissas of these plots are given in terms of yaw. (a) Ratios to the values at −1.5° yaw. The ratios are fitted to a fourth-order polynomial. The fitted curve is hidden by the data points. (b) The fitted curve from Fig. 12(a). The maximum value for the curve is 1.001 at a yaw angle of −0.8°. For use as a correction factor, the curve is normalized to a maximum value of unity.

Table 2. Characteristics of the Fourth-Order Polynomial Curves Used to Describe the Yaw-Angle Dependence of the SeaWiFS Diffuser Assembly[a]

SeaWiFS Band	Maximum Value of the Fitted Curve (dimensionless)	Yaw Angle of the Maximum Value (deg)
1	1.00086	−0.85
2	1.00101	−0.82
3	1.00112	−0.78
4	1.00121	−0.77
5	1.00112	−0.77
6	1.00116	−0.66
7	1.00168	−0.43
8	1.00242	−0.14

[a]The curves are normalized to maximum values of unity before they are applied as corrections to the measurements on orbit.

transfer-to-orbit experiment.[12] On day 72, there was a problem with the constants for orbit determination uplinked to the satellite, which caused the satellite computer to shut down and go into safe haven. On day 80 after launch, regular solar measurements were restarted. There is no seamless transition in the solar diffuser measurements from day 72 to day 80 after launch, although the differences at the ends of the data gap are small.[12] The causes of these differences are not immediately obvious from the data set. For this reason, the data from day 46 to day 72 after launch are considered the best representatives for the trend in the diffuser measurements for the initial phase of on-orbit operation. And, as such, they provide the best basis for extrapolations to estimate the changes from the launch date to the start of solar diffuser measurements on day 46.

From day 80 to day 800 after launch, the measurement results are fitted to a ninth-order polynomial curve to smooth the time series, while the basic structure is maintained in the time-dependent changes. This is the second part of the fitted curve. There is no theoretical basis behind the choice of this order polynomial; however, as with Fig. 13(a) for band 1, the fitted curves for all eight bands lie within the scatter of the data. As stated above, only the first 400 days after launch are used in the reflectance-based calibration, whereas the fitted curves extend to 800 days. This truncation was designed, in part, to remove the curved tails that sometimes occur at the end points of polynomial fits. Such a tail is present in Fig. 13(b) from day 770 after launch to day 800.

For each band, the two parts of the fitted curve are joined at the point (in days after launch) where the two parts intersect. For band 1 (Fig. 13), the intersection occurs on day 84 after launch. The average intersection point is 80 days after launch. In each case, the two parts of the fitted curve join together smoothly; that is to say, the change in slope of the fitted curve is small around the intersection point, as shown in Fig. 13.

6. Gain Ratios

For measurements of the Earth (Earth mode), the DNs from the detectors are recorded over the range of telescope angles of ±58° about Earth nadir. For calibration measurements (solar mode), DNs from the detectors are recorded over the range of 60–175 deg from Earth nadir, with the solar diffuser measurements centered on the telescope angle of 90° from nadir. At an angle of 107°, the telescope rotates past the aperture of the solar diffuser, and the instrument views the dark interior of the instrument housing for the next 158° of telescope rotation.[17]

Over a portion of the region where the telescope views the dark interior of the housing, the zero offsets for the instrument bands are determined. These values are applied to each scan from the instrument, whether in Earth or solar mode. They are inserted into each scan line from the instrument as the first datum and are subtracted from the measurements during ground processing.

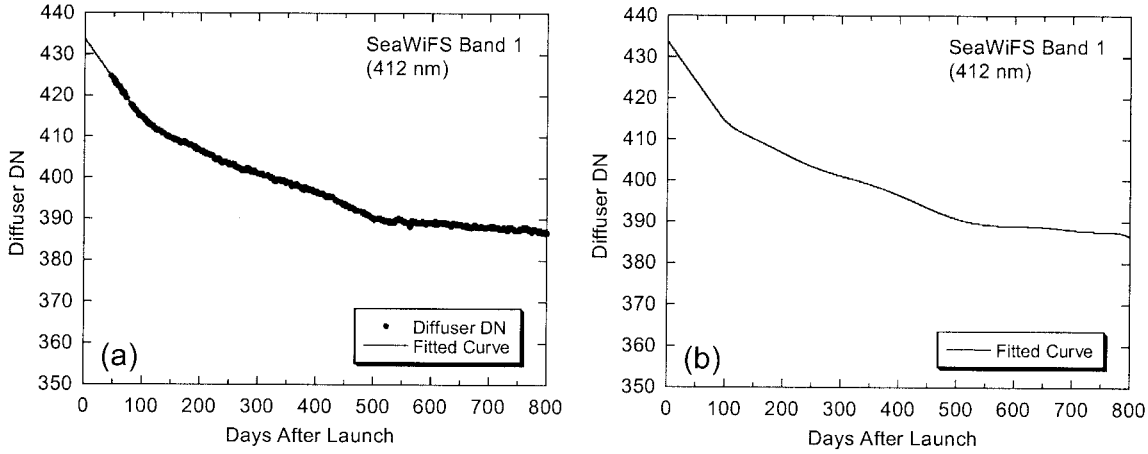

Fig. 13. Band 1 solar diffuser measurements corrected for the effects of yaw-angle changes. In addition, the effects of the Earth–Sun distance and the changes in the long-term instrument response were removed. The results were fitted to two curves: a first-order polynomial from day zero to day 75; and a ninth-order polynomial for day 75 and longer. (a) Measured results and the fitted curves. For most of the panel, the fitted curves are hidden by the data points. (b) Fitted curves from Fig. 13(a).

For measurements in the solar mode, a calibration pulse is applied during a portion of the scan of the interior of the instrument housing, at angles from 125° to 135° from Earth nadir. For each band, the calibration pulse is a voltage that is generated with a zener diode and a resistor. This voltage is constant from scan line to scan line, and it is applied at the output of the transimpedance amplifier (current-to-voltage converter) for the photodiode. Because the photodiode is in the dark, its output is zero. The calibration pulse is inserted before the intermediate amplifier, which has the circuitry that determines the electrical gain.

For each SeaWiFS band, there are four electronic gains. Gain 1 is the standard gain for Earth measurements. Gain 2 has approximately twice the sensitivity (radiance units per DN) as gain 1. It has been designed to replace gain 1 if the radiometric sensitivity of the band has decreased to the point that the Earth measurements are quantization limited, that is, to the point where the DNs for the Earth measurements have become too small. At present, it is anticipated that gain 2 will never be used by SeaWiFS. Gain 3 has been designed for measurements of the Sun by use of the diffuser, and gain 4 has been designed for measurements of the Moon. However, for SeaWiFS band 2, measurements of the solar diffuser are best made with the standard gain for Earth measurements, gain 1.

For each band, measurements of an internally generated electronic calibration pulse provide DNs for a series of instrument configurations, including each of the gains for the band.[17] In the same manner as measurements of input spectral radiances, each DN value for the calibration pulse is corrected for the zero offset of the measurement. For each band, the gain ratios are calculated as the DN for each gain relative to the DN from the standard gain, gain 1. For the SeaWiFS solar measurements, the gain ratios for the eight bands are shown in Fig. 14.

7. Calibration Coefficients

In the laboratory, a pressed PTFE plaque was used as a calibration standard, and the SeaWiFS instrument, acting as a transfer radiometer, transferred the reflectance of the plaque to the flight diffuser. On orbit, the conditions of the laboratory characterization have been duplicated, as closely as possible, and deviations from those conditions have been corrected, again as closely as possible. This allows use of the SeaWiFS radiometer as a transfer instrument a second time, this time from the flight diffuser to the Earth, which the instrument views as a source of reflected sunlight. The long-term changes in the reflectance of the flight diffuser and in the gain ratios for the solar measurements are slowly changing functions of time, which can be incorporated into the instrument calibration equation.

For SeaWiFS, the principal TOA reflectance product is the bidirectional reflectance factor (BRF) $R_E(t)$. The BRF is defined as the ratio of the radiant flux from a sample surface to that of an ideal diffuse standard surface irradiated in the same way as the sample.[18,19] For an ideal diffuse surface,[18,19] the BRDF has a value of $1/\pi$ sr^{-1}, and its BRF, by definition, is unity (dimensionless). Thus, for an ideal diffuse surface and for other surfaces as well, the conversion constant between BRDF and BRF has a value of π steradians.

The BRF is the standard reflectance product for imaging of the Earth's surface by satellite instruments such as the Advanced Very High Resolution Radiometer (AVHRR)[20] and the moderate-resolution imaging spectroradiometer (MODIS).[21] The SeaWiFS TOA BRFs are also corrected for the cosine of the zenith angle. This correction accounts for the effect of the projection of the solar irradiance when it is not normal to the Earth's surface. This effect is fundamental to all reflectance measurements where the radiant flux from the surface overfills the field of view of the instrument. The equation that converts Earth-measured digital numbers (DN_E) into BRFs is

$$\begin{aligned} R_E(t) &= \pi F_E(t) \\ &= [\mathrm{DN}(t) - \mathrm{DN}_0(t)]_E \frac{D_{\mathrm{ES}}{}^2(t)}{\cos(\theta_I)} [\pi k_F(t_0)]\alpha(t_0) \\ &\quad \times [\Delta_G(t)]^{-1}[\Delta_F(t)]^{-1}, \end{aligned} \tag{10}$$

where $F_E(t)$ is the Earth BRDF, $[\mathrm{DN}(t) - \mathrm{DN}_0(t)]_E$ are the Earth-view DNs corrected for instrument effects, $D_{\mathrm{ES}}(t)$ is the Earth–Sun distance (in AU), and t is the time (in days) after the launch of SeaWiFS. The term $\cos(\theta_I)$ is the cosine of the incident zenith angle θ_I at time t. For Earth measurements of reflected sunlight, θ_I is the solar zenith angle. During the laboratory characterization of the SeaWiFS diffuser, the effect of the incidence angle of the irradiance on the reference PTFE diffuser at the instrument's Earth aperture was also a factor. However, in the laboratory measurement, the irradiance was normal to the surface of the PTFE diffuser, and the cosine of the incidence angle was unity.

In Eq. (10), the term $k_F(t_0)$ is the reflectance calibration coefficient at the time of the SeaWiFS launch (t_0). The coefficient is given in terms of the BRDF per DN (sr^{-1} DN^{-1}), and the value of π steradians converts the coefficient into the BRF. The terms $[\Delta_F(t)]^{-1}$ and $[\Delta_G(t)]^{-1}$ give the corrections for the changes in the reflectance of the diffuser and the gain ratio, respectively, over time. For each SeaWiFS band, the time dependence for the diffuser reflectance over the 400 days after the launch of SeaWiFS is given in Fig. 15. The correction is the reciprocal of that time dependence. And as shown in Fig. 14, the relative changes for the gain ratios are small, of the order of a few tenths of a percent. For use in Eq. (10), the gain ratios from Fig. 14 were normalized to unity at the launch date to provide the values for $\Delta_G(t)$.

The reflectance properties of the Earth's surface and the atmosphere above it are complicated functions of the incident azimuthal and elevation angles of the solar irradiance (ϕ_I and θ_I) and of the scattered

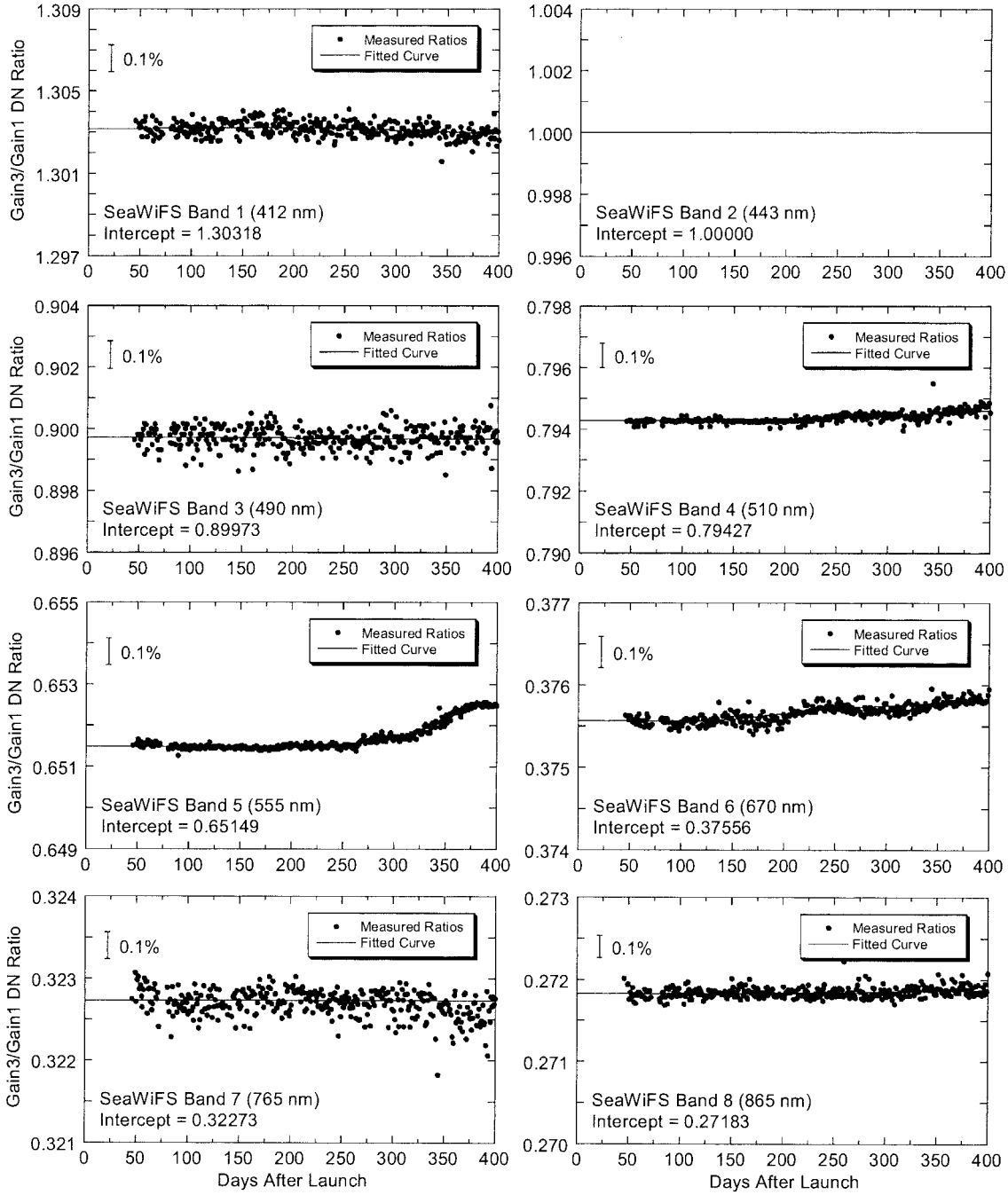

Fig. 14. Gain ratios for the SeaWiFS solar measurements for the 400 days after launch. For band 2, the solar measurements are made at the standard gain for Earth measurements, gain 1. For the other bands, the measurements are made at gain 3. For each band, the ratios are determined from measurements of an internally generated electronic calibration pulse.

radiance (ϕ_S and θ_S). This is true of all reflecting surfaces.[12] As a result, the Earth reflectance term $R_E(t)$ contains the effects of these surface and atmospheric properties. The angles can be calculated from knowledge of the positions of the spacecraft, the Earth, and the Sun in a standard frame of reference for each Earth measurement, but the determination of the properties is outside of the calculation of $R_E(t)$. In addition, because each SeaWiFS band has a finite bandwidth, the measured reflectances must be considered as averages over these bandwidths.[12] The BRDF of the instrument diffuser varies smoothly and slowly with wavelength; however, any wavelength-dependent structure of the effective reflectance of the Earth's surface within the instrument's bandwidth is not known from these measurements.

The corrections to the Earth-view DNs in Eq. (10) include the standard instrumental corrections for SeaWiFS measurements on orbit.[9] However, the effect of the Earth–Sun distance is not a part of the standard procedure because it is not an effect arising from the internal operation of the instrument. For

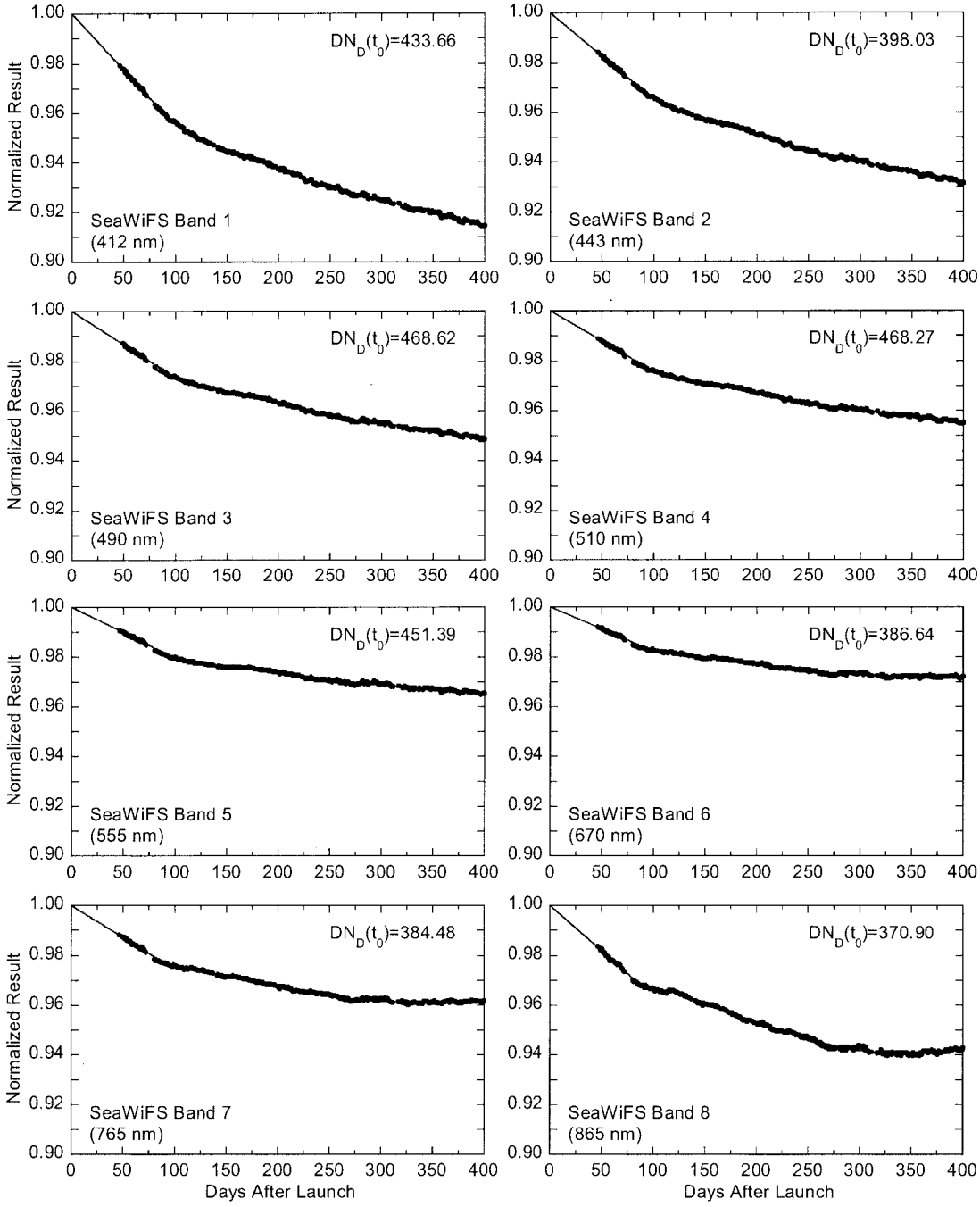

Fig. 15. Diffuser reflectance changes for the 400 days after the SeaWiFS launch. The values in each panel are normalized to unity at the launch date, and each panel contains the DN at the launch date.

this reason, the Earth–Sun distance correction $D_{ES}^2(t)$ is included as a separate term in Eq. (10), making the processing of the Earth-view and diffuser-view DNs identical.

The term $\alpha(t_0)$ in Eq. (10) is applied as an initialization constant determined from surface-truth measurements by the Marine Optical Buoy (MOBY).[22] It has no time dependence, and it is dimensionless. The term is used in the standard processing stream for ocean color measurements, which are the primary products for SeaWiFS measurements. The initialization constant is required for the particular characteristics of ocean measurements, where the ocean is relatively dark and most of the TOA radiance comes from the atmosphere.[22] For land and atmosphere applications and for the TOA BRF, $\alpha(t_0)$ is set to unity.[4]

It is important to emphasize that $\alpha(t_0)$ is provided by a vicarious calibration[22] in a process that is separate from the determination of the other coefficients in Eq. (10). It is not part of the on-orbit reflectance-based calibration of the instrument, and it is used

Table 3. Components of the Calculation of the Calibration Coefficient $k_F(t_0)$

SeaWiFS Band	$F_D(t_0)$ (sr^{-1})	$DN_D(t_0)$ (dimensionless)	$G_R(t_0)$ (dimensionless)	$k_F(t_0)$ (sr^{-1} DN^{-1})
1	0.0269	433.66	1.30318	0.0000808
2	0.0279	398.03	1.00000	0.0000701
3	0.0274	468.62	0.89973	0.0000526
4	0.0279	468.27	0.79427	0.0000473
5	0.0274	451.39	0.65149	0.0000395
6	0.0277	386.64	0.37556	0.00002691
7	0.0281	384.48	0.32273	0.00002359
8	0.0297	370.90	0.27183	0.00002177

only in the production of the ocean color data products. As a result, for the applications in this section, $\alpha(t_0)$ is also given a value of unity.

The calibration coefficient $k_F(t_0)$ is written as

$$k_F(t_0) = \frac{F_D(t_0)}{DN_D(t_0)[G_R(t_0)]^{-1}}, \tag{11}$$

where $F_D(t_0)$ is the BRDF from Table 3, $DN_D(t_0)$ is the diffuser DN at the launch date from Fig. 15, and $G_R(t_0)$ is the gain ratio at the launch date from Fig. 14. At the SeaWiFS launch date, Eq. (10) reduces to

$$\frac{F_E(t_0)}{DN_E(t_0)} \frac{\cos(\theta_I)}{D_{ES}{}^2(t_0)} = \frac{F_D(t_0)}{DN_D(t_0)} \frac{1}{[G_R(t_0)]^{-1}}, \tag{12}$$

where both sides of the equation contain the ratio of the BRDF to the DNs in the measurement. The left-hand side of Eq. (12) has corrections for the solar zenith angle and the Earth–Sun distance. Both of these corrections were made in the calculation of $DN_D(t_0)$ on the right-hand-side of Eq. (12). However, $DN_D(t_0)$ must be corrected back to gain 1, which is the electronic gain for measurements of the Earth. Equation (12) can also be given in terms of BRF when we multiply both sides by π steradians. The solar irradiance is a fundamental component of SeaWiFS measurements of the Earth and of the diffuser. However, it cancels from Eq. (12) because it is assumed that the irradiance is constant over the length of day t_0. In a similar manner, the solar irradiance cancels from Eq. (10) because it is also assumed to remain constant over the first 400 days of SeaWiFS operations on orbit. And in a similar manner, the assumption of a constant solar irradiance is fundamental to use of the Moon to determine changes in the SeaWiFS instrument itself.[4] And, in an even broader sense, the assumption is fundamental for use of remote sensing from space to detect changes in the Earth over time.[23]

The reflectance-to-DNs ratio at the time of launch is established as a calibration coefficient in the same manner as calibration coefficients for radiance are set up in the laboratory. There, the instrument views a calibrated radiance, and the measured DNs provide the denominator of the coefficient. However, for the reflectance characterization in the laboratory, the solar irradiance was not available, so the calibration coefficient was determined for the day that SeaWiFS entered orbit.

For the SeaWiFS instrument, measurements of the Moon provide the basis for determining changes in the instrument's radiometric sensitivity. This is expressed in the standard calibration equation for TOA radiance $L_T(t)$ from Eq. (13) of Barnes *et al.*[4]:

$$L_T(t) = [DN(t) - DN_0(t)]_E k_2(t_0)\alpha(t_0) \times \{1 - \beta[1 - \gamma \exp(-\delta t)]\}^{-1}, \tag{13}$$

where $k_2(t_0)$ is the prelaunch radiometric calibration coefficient (in mW cm^{-2} sr^{-1} μm^{-1} DN^{-1}), β and γ are dimensionless, and δ has the units of day^{-1}. The value of γ is within a few percent of unity. The values of β, γ, and δ are fitted parameters derived from lunar measurements by SeaWiFS.[4] In an exponential manner, this lunar-based sensitivity factor decreases fractionally from a value of unity at t_0 to a value of $(1 - \beta)$ for times far into the future. The correction for the change in radiometric sensitivity is applied as the reciprocal of the exponential change term.

As explained above, the changes in the diffuser reflectance cannot be known as well as the changes in the SeaWiFS instrument itself. As shown in Section 5, the change in the instrument's radiometric sensitivity $\{1 - \beta[1 - \gamma \exp(-\delta t)]\}$ is a part of the calculation of $\Delta_F(t)$. This knowledge allows the instrument change correction in Eq. (13) to be substituted for the reflectance and gain ratio change factors in Eq. (10). When this approach is taken, Eq. (10) becomes

$$R_E(t) = \pi F_E(t) = [DN(t) - DN_0(t)]_E \frac{D_{ES}{}^2(t)}{\cos(\theta_I)} [\pi k_F(t_0)]\alpha(t_0) \times \{1 - \beta[1 - \gamma \exp(-\delta t)]\}^{-1}. \tag{14}$$

The change coefficients β, γ, and δ are the same as those in Eq. (13), and the other terms in Eq. (14) have counterparts in Eq. (10).

As a calibration equation, Eq. (14) is not limited to the first 400 days after launch, as is Eq. (10), with its limitations on the duration of the time series for $\Delta_F(t)$ and $\Delta_G(t)$ from Sections 5 and 6. In addition, Eq. (14) gives a better correction for instrument change during the first 400 days than does Eq. (10). However, the analyses in Sections 5 and 6 are fundamental to the reflectance-based calibration because they determine the values $DN_D(t_0)$ and $G_R(t_0)$ for the calculation of the calibration coefficient $k_F(t_0)$.

8. Concluding Remarks

The SeaWiFS transfer-to-orbit experiment[12] was based on a prediction of the DNs from the instrument at the time of the insertion of the instrument into orbit. In that experiment, there were minimal corrections to the DNs from orbit. There were no corrections for the temperatures of the focal planes or for the yaw angle of the on-orbit measurements. These

Table 4. Comparison of the Values of $DN_D(t_0)$ with Those Predicted for the Transfer-to-Orbit Experiment[a]

SeaWiFS Band	DN_P (dimensionless)	$D_{ES}^2(t_0)$ (dimensionless)	DN_{CORR} (dimensionless)	$DN_D(t_0)$ (dimensionless)	Ratio (dimensionless)
1	428.9	1.03023	441.8	433.66	0.982
2	385.1	1.03023	396.7	398.03	1.003
3	451.0	1.03023	464.5	468.62	1.009
4	455.9	1.03023	469.6	468.27	0.997
5	438.9	1.03023	452.1	451.39	0.998
6	380.6	1.03023	392.0	386.64	0.986
7	375.5	1.03023	386.8	384.48	0.994
8	366.0	1.03023	377.0	370.90	0.984
Mean					0.994
Standard deviation					0.010

[a]The Earth–Sun distance correction $D_{ES}^2(t_0)$ is applied to the predicted digital numbers (DN_P) to provide a corrected set of predicted digital numbers (DN_{CORR}). This is necessary because of a difference in the calculation procedures for DN_P and $DN_D(t_0)$. See text for details.

corrections were included in the uncertainties for that experiment, and they were considered small with respect to the uncertainty in the atmospheric transmittance for the ground measurements.[12] The measurement results for $DN_D(t_0)$ in Table 3 include the on-orbit instrumental effects. As such, they provide an update to the results of the transfer-to-orbit experiment. In addition, the updated comparison of the predicted values for the start of the SeaWiFS mission and of their measured counterparts for the same time is shown in Table 4.

For the transfer-to-orbit experiment, the effect of the Earth–Sun distance was applied to the predicted digital numbers DN_P [see Eq. (14) of Barnes *et al.*[12]]. This was done to eliminate the need for this correction to the measured DNs from orbit. Thus, for the transfer-to-orbit experiment,[12] the measurements from orbit were reported without the Earth–Sun distance correction. Because the Earth–Sun distance was 1.015 AU at the start of the SeaWiFS mission on orbit, the predicted DNs for the transfer-to-orbit experiment (DN_P) were reduced by 3%. However, the values for $DN_D(t_0)$ in Tables 3 and 4 have a correction for the Earth–Sun distance included in their calculation (see Section 5). They are corrected to an Earth–Sun distance of 1 AU. Thus the 3% correction to DN_P in the transfer-to-orbit calculations becomes redundant here. This is the reason for the $D_{ES}^2(t_0)$ factor in Table 4 and the 3% increase in the values for DN_{CORR} relative to DN_P.

The results in Table 4 show the measured DNs to average 0.6% lower than the predicted values with a standard deviation of 1.0%. For the transfer-to-orbit experiment, the measured DNs averaged 0.8% higher than the predicted values with a standard deviation of 0.9%.[12] In both cases, the results fall within the 3% uncertainty of the experiment. Thus the results of the reflectance calibration of SeaWiFS presented here do not change the basic results of the transfer-to-orbit experiment from Barnes *et al.*[12]

Other Earth-observing satellite sensors use their solar diffusers as the basis for the radiance-based calibration of their measurements.[24,25] This type of calibration requires a knowledge of the characterization of the diffuser plus knowledge of the magnitude of the solar spectral irradiance to provide a reference spectral radiance from the surface of the diffuser. Thus, with use of a solar irradiance model, it is also possible to use the reflectance-based calibration of SeaWiFS as the basis for a radiance-based calibration of the instrument at the start of on-orbit operations. In addition, there are three other prelaunch radiance-based calibrations of SeaWiFS. The first is based on measurements of an integrating sphere by the instrument manufacturer in 1993[26]; the second is based on measurements of a different integrating sphere four months before the launch of SeaWiFS in 1997[3]; and the third is the prelaunch SeaWiFS solar radiation-based calibration[5,6] performed outdoors at the instrument manufacturer's facility with the Sun used as the light source. For SeaWiFS, the calibration in 1997, just before launch, is the basis for the instrument's on-orbit calibration.[4] The internal consistency of these four radiance-based calibration techniques is discussed in the companion paper.[27]

Finally, one of the most fundamental land products derived from satellite measurements is the normalized difference vegetation index (NDVI). The index is based on the reflectance of chlorophyll pigment in the visible and near-infrared portion of the electromagnetic spectrum. Green leaves have a reflectance of less than 20% in the wavelength region from 500 to 700 nm, but approximately 60% in the range from 700 to 1300 nm.[28] The differential reflectance in these two wavelength regions can be used to derive many data products, ranging from land cover classification[29] to net primary production by the photosynthetic biosphere.[30] For the most recent reprocessing of the SeaWiFS data set (reprocessing 4, June 2002), a NDVI product has been added to the set of standard SeaWiFS data products. For SeaWiFS, NDVI is calculated from the surface BRFs of the 670- and 865-nm bands by the equation

$$\mathrm{NDVI} = \frac{R_S(865) - R_S(670)}{R_S(865) + R_S(670)}, \tag{15}$$

where $R_S(865)$ is the surface BRF at 865 nm, that is, the TOA reflectance corrected for atmospheric effects. For land products, the approximation to the surface BRF is derived when we correct for the effects of light absorption by atmospheric gases including ozone and water vapor and for atmospheric molecular scattering. For SeaWiFS land measurements, there is no correction for the effects of atmospheric aerosols.

The SeaWiFS Project is currently working on the implementation of the enhanced vegetation index (EVI) used by the MODIS Science Team.[31] This index is an empirically modified NDVI that uses a blue band (at 443 nm) as a correction to the red band for atmospheric aerosol scattering. The EVI equation takes the form

$$\mathrm{EVI} = \frac{R_S(865) - R_S(670)}{R_S(865) + [C_1 R_S(670) - C_2 R_S(443)] + L} \times (1 + L), \quad (16)$$

where C_1 and C_2 have values of 6.0 and 7.5, respectively. The EVI also contains an empirically derived adjustment factor L for surface effects, such as the reflectance of soil in the measured sample. The value for L is unity. Currently, the EVI is a test product by the SeaWiFS Project. However, the MODIS Science Team has used SeaWiFS measurements to test their vegetation indices.[32] In addition, SeaWiFS has the capability of producing a similar three-band vegetation index proposed for use by the MERIS (medium resolution imaging spectrometer) Project.[33]

The reflectance-based calibration of SeaWiFS provides a natural starting point for these vegetation indices. However, SeaWiFS was developed as an ocean color imager, with a primary geophysical product of water-leaving radiance. As a result, the principal calibration product for SeaWiFS is TOA radiance, based on a prelaunch calibration with an integrating sphere.[4] For this calibration, the conversion to a TOA BRF requires use of a solar irradiance model, which incorporates an additional source of uncertainty in the reflectance product. The project currently (reprocessing 4, June 2002) uses the solar model of Neckel and Labs[34] to convert TOA radiance to reflectance. Testing of the reflectance-based calibration presented here for use in the next SeaWiFS reprocessing is under way.

This research was supported by the SeaWiFS Project under NASA contract NAS5-00141 (R. A. Barnes) and by the SIMBIOS (Sensor Intercomparison and Merger for Biological and Interdisciplinary Oceanic Studies) Project under NASA contract NAS5-00197 (E. F. Zalewski).

References

1. A. Morel and B. Gentili, "Diffuse reflectance of oceanic waters: its dependence on Sun angle as influenced by the molecular scattering contribution," Appl. Opt. **30,** 4427–4438 (1991).
2. A. Morel and B. Gentili, "Diffuse reflectance of oceanic waters. II. Bidirectional aspects," Appl. Opt. **32,** 6864–6879 (1993).
3. B. C. Johnson, E. A. Early, R. E. Eplee, Jr., R. A. Barnes, and R. T. Caffrey, *The 1997 Prelaunch Calibration of SeaWiFS*, NASA Tech. Memo. 1999-206892, Vol. 4, S. B. Hooker and E. R. Firestone, eds. (NASA Goddard Space Flight Center, Greenbelt, Md., 1999).
4. R. A. Barnes, R. E. Eplee, Jr., G. M. Schmidt, F. S. Patt, and C. R. McClain, "Calibration of SeaWiFS. I. Direct techniques," Appl. Opt. **40,** 6682–6700 (2001).
5. S. F. Biggar, K. J. Thome, P. N. Slater, A. W. Holmes, and R. A. Barnes, "Second SeaWiFS preflight solar-radiation-based calibration experiment," in *SeaWiFS Calibration Topics, Part 1*, NASA Tech. Memo. 104566, Vol. 27, S. B. Hooker, E. R. Firestone, and J. G. Acker, eds. (NASA Goddard Space Flight Center, Greenbelt, Md., 1997), pp. 20–24.
6. R. A. Barnes, R. E. Eplee, Jr., S. F. Biggar, K. J. Thome, E. F. Zalewski, P. N. Slater, and A. W. Holmes, *The SeaWiFS Solar Radiation-Based Calibration and the Transfer-to-Orbit Experiment*, NASA Tech. Memo. 1999-206892, Vol. 5, S. B. Hooker and E. R. Firestone, eds. (NASA Goddard Space Flight Center, Greenbelt, Md., 1999).
7. C. Fröhlich, "Observations of irradiance variation," Space Sci. Rev. **94,** 15–24 (2000).
8. R. A. Barnes, W. L. Barnes, W. E. Esaias, and C. R. McClain, *Prelaunch Acceptance Report for the SeaWiFS Radiometer*, NASA Tech. Memo. 104566, Vol. 22, S. B. Hooker, E. R. Firestone, and J. G. Acker, eds. (NASA Goddard Space Flight Center, Greenbelt, Md., 1994).
9. R. A. Barnes, A. W. Holmes, W. L. Barnes, W. E. Esaias, C. R. McClain, and T. Svitek, *SeaWiFS Prelaunch Radiometric Calibration and Spectral Characterization*, NASA Tech. Memo. 104566, Vol. 23, S. B. Hooker, E. R. Firestone, and J. G. Acker, eds. (NASA Goddard Space Flight Center, Greenbelt, Md., 1994).
10. R. A. Barnes and R. E. Eplee, "The SeaWiFS solar diffuser," in *SeaWiFS Calibration Topics, Part 1*, NASA Tech. Memo. 104566, Vol. 39, S. B. Hooker, E. R. Firestone, and J. G. Acker, eds. (NASA Goddard Space Flight Center, Greenbelt, Md., 1996), pp. 54–61.
11. Hughes Santa Barbara Research Center (now Raytheon Santa Barbara Remote Sensing), SeaWiFS Critical Design Review, 18–19 December 1991 (Santa Barbara Research Center, Goleta, Calif., 1991).
12. R. A. Barnes, R. E. Eplee, Jr., S. F. Biggar, K. J. Thome, E. F. Zalewski, P. N. Slater, and A. W. Holmes, "SeaWiFS transfer-to-orbit experiment," Appl. Opt. **39,** 5620–5631 (2000).
13. V. R. Weidner and J. J. Hsia, "Reflection properties of pressed polytetrafluoroethylene powder," J. Opt. Soc. Am. **71,** 856–861 (1981).
14. J. J. Hsia and V. R. Weidner, "NBS 45-degree/normal reflectometer for absolute reflectance factors," Metrologia **17,** 97–102 (1981).
15. E. A. Early, P. Y. Barnes, B. C. Johnson, J. J. Butler, C. J. Bruegge, S. F. Biggar, P. R. Spyak, and M. M. Pavlov, "Bidirectional reflectance round-robin in support of the Earth Observing System program," J. Atmos. Oceanic Technol. **17,** 1077–1091 (2000).
16. J. M. Palmer and P. N. Slater, "A ratioing radiometer for use with a solar diffuser," in *Calibration of Passive Remote Observing Optical and Microwave Instrumentation*, B. G. Guenther, ed., Proc. SPIE **1493,** 106–117 (1991).
17. R. H. Woodward, R. A. Barnes, C. R. McClain, W. E. Esaias, W. L. Barnes, and A. T. Mecherikunnel, *Modeling of the SeaWiFS Solar and Lunar Observations*, NASA Tech. Memo. 104566, Vol. 10, S. B. Hooker and E. R. Firestone, eds. (NASA Goddard Space Flight Center, Greenbelt, Md., 1993).
18. F. E. Nicodemus, J. C. Richmond, J. J. Hsia, I. W. Ginsberg, and T. Limperis, "Geometrical considerations and nomenclature for reflectance," NBS Monogr. 160 (National Bureau of Standards, Washington D.C., 1977).
19. P. Y. Barnes, E. A. Early, and A. C. Paar, "Spectral reflec-

tance," NIST Special Publ. SP 250-48 (National Institute of Standards and Technology, Gaithersburg, Md., 1998).
20. C. R. N. Rao, "Pre-launch calibration of channels 1 and 2 of the Advanced Very High Resolution Radiometer," NOAA Tech. Rep. NESDIS 36 (National Oceanic and Atmospheric Administration, Washington, D.C., 1987).
21. B. Guenther, W. Barnes, E. Knight, J. Barker, J. Harnden, R. Weber, M. Roberto, G. Godden, H. Montgomery, and P. Abel, "MODIS calibration: a brief review of the strategy for the at-launch calibration," J. Atmos. Oceanic Technol. **13,** 274–285 (1996).
22. R. E. Eplee, Jr., W. D. Robinson, S. W. Bailey, D. K. Clark, P. J. Werdell, M. Wang, R. A. Barnes, and C. R. McClain, "Calibration of SeaWiFS. II. Vicarious techniques," Appl. Opt. **40,** 6701–6718 (2001).
23. C. Fröhlich and J. Lean, "The sun's total irradiance: cycles, trends and related climate change uncertainties since 1976," Geophys. Res. Lett. **25,** 4377–4380 (1998).
24. B. L. Markham, W. C. Boncyk, D. L. Helder, and J. L. Barker, "Landsat-7 Enhanced Thematic Mapper Plus radiometric calibration," Can. J. Remote Sens. **23,** 318–332 (1997).
25. J. Nieke, I. Asanuma, K. Tanaka, and Y. Tange, "Global Imager's on-board calibration (VNIR-SWIR)," in *Earth Observing Systems VI*, W. L. Barnes, ed., Proc. SPIE **4483,** 231–241 (2002).
26. R. A. Barnes and R. E. Eplee, Jr., "The 1993 SeaWiFS calibration using band-averaged spectral radiances," in *SeaWiFS Calibration Topics, Part 2*, NASA Tech. Memo. 104566, Vol. 40, S. B. Hooker and E. R. Firestone, eds. (NASA Goddard Space Flight Center, Greenbelt, Md., 1997), pp. 39–47.
27. R. A. Barnes and E. F. Zalewski, "Reflectance-based calibration of SeaWiFS. II. Conversion to radiance," Appl. Opt. **42,** 1648–1660 (2003).
28. NOAA, NOAA Global Vegetation Index (GVI) User's Guide, (National Oceanic and Atmospheric Administration, Camp Springs, Md., 1997); see http://www2.ncdc.noaa.goc/docs/gviug/index.htm.
29. C. J. Tucker, J. R. G. Townshend, and T. E. Goff, "African land-cover classification using satellite data," Science **227,** 369–375 (1985).
30. M. J. Behrenfeld, J. T. Randerson, C. R. McClain, G. C. Feldman, S. O. Los, C. J. Tucker, P. G. Falkowski, C. B. Field, R. Frouin, W. E. Esaias, D. D. Kolber, and N. H. Pollack, "Biospheric primary production during an ENSO transition," Science **291,** 2594–2597 (2001).
31. C. O. Justice, E. Vermote, J. R. G. Townshend, R. Defries, D. P. Roy, D. K. Hall, V. V. Salomonson, J. L. Privette, G. Riggs, A. Strahler, W. Lucht, R. B. Myneni, Y. Knyazikhin, S. W. Running, R. R. Nemani, Z. Wan, A. R. Huete, W. van Leeuwen, R. E. Wolfe, L. Giglio, J.-P. Muller, P. Lewis, and M. J. Barnsley, "The Moderate Resolution Imaging Spectroradiometer (MODIS): land remote sensing for global change research," IEEE Trans. Geosci. Remote Sens. **36,** 1228–1249 (1998).
32. W. J. D. van Leeuwen, A. R. Huete, and T. Liang, "Evaluation of the MODIS vegetation index algorithm using SeaWiFS data," in IGARSS '98: *1998 IEEE International Geoscience and Remote Sensing Symposium on Sensing and Managing the Environment*, T. I. Stein, ed. (Institute of Electrical and Electronics Engineers, New York, 1999), pp. 1445–1447.
33. N. Gobron, B. Pinty, M. Verstraete, and Y. Govaerts, "The MERIS global vegetation index (MGVI): description and preliminary application," Int. J. Remote Sens. **20,** 1917–1927 (1999).
34. H. Neckel and D. Labs, "The solar radiation between 3300 and 12500 Å," Sol. Phys. **90,** 205–258 (1984).